Journal of NAMP 72, (2026) 23-36

The Nigerian Association of Mathematical Physics

Journal homepage: https://nampjournals.org.ng

EIGEN SOLUTION AND THERMODYNAMIC PROPERTIES OF NONRELATIVISTIC SYSTEM UNDER THE INVERSELY QUADRATIC VARSHINI POTENTIAL

[*1]Imrana, M. H., [2]Teru, P. B., [3]Ngari, A. Z., [1]Yabagi, J. A., [1]Ndanusa, B., [4]Gyobe, A. M., [5]Ndom, N. B., and [6]Naibi, A. B

[1]Department of Physics, Ibrahim Badamasi Babangida University, Lapai, Nigeria.
[2]Department of Physics, University of Maiduguri, Nigeria.
[3]Department of Physics, Nigerian Army University, Biu, Nigeria.
[4]Department of Physics, Nigeria Maritime University of Okeronkoko, Nigeria.
[5]Air force Institute of Technology, Kaduna, Nigeria.
[6]Department of Basic Science, Niger State College of Agriculture Mokwa, Nigeria.

ARTICLE INFO

Article history:
Received xxxxx
Revised xxxxx
Accepted xxxxx
Available online xxxxx

Keywords:
Nonrelativistic System;
Inversely Quadratic Varshini Potential;
NUFA Method;
Eigen Solution.

ABSTRACT

Approximate analytical solutions of the Schrödinger equation are presented using a newly proposed Inversely Quadratic Varshini Potential (IQVP), developed as a modification of the Varshini potential. Using the Nikiforov–Uvarov functional analysis method, the energy eigenvalues and wave functions are determined. These solutions are employed to compute vibrational thermodynamic quantities. The thermodynamic trends agree well with existing literature, and numerical results are reported. The results may have potential applications in atomic, molecular, and nuclear physics.

1. INTRODUCTION

As a second-order differential equation, the Schrödinger equation serves as a cornerstone of quantum mechanics, enabling the analysis of quantum systems under diverse potential models and finding applications across atomic, molecular, and nuclear domains [1, 2]. From the Schrödinger equation, one can obtain the energy eigenvalues and corresponding wave functions, which provide a complete description of the quantum mechanical behavior of the system [3]. In nonrelativistic quantum mechanics, both exact and approximate solutions of the Schrödinger wave equation are highly significant, since the corresponding wave functions and energy eigenvalues contain

[*]Corresponding author: IMRANA, M. H
E-mail address: oyelamioyewole@gmail.com
https://doi.org/10.60787/jnamp.vol72no.660

essential information relevant to the characterization of diverse quantum systems, encompassing atomic structure theory, quantum chemistry, and quantum electrodynamics [4, 5]. The remarkable experimental success of the Schrödinger wave equation has inspired extensive use of various analytical methods to solve the radial Schrödinger equation. Considerable research has been carried out on solving the Schrödinger and Klein–Gordon equations for a variety of interaction potentials. For instance, Imrana *et al.* [6] investigated the Schrödinger equation with the Varshni–Hellmann potential (VHP) in the presence of external magnetic and Aharonov–Bohm fields using the NUFA method, and derived the magnetization, magnetic susceptibility, and other thermodynamic properties at both zero and finite temperatures. Similarly, Tazimi [7] derived the bound-state solutions of the Schrödinger equation with the Varshni-Hellmann potential by applying the ansatz approach. William *et al.* [8] explored the Hulthén and Hellmann potentials, with the latter arising from Hellmann's study of the Schrödinger equation involving a linear combination of Coulomb and Yukawa interactions [9]. The Varshni potential, which characterizes repulsive short-range interactions, has been analyzed within the Schrödinger equation formalism and has played a significant role in advancing research in chemical and nuclear physics [10, 11]. This study addresses the radial Schrödinger equation for a newly introduced potential, derived by incorporating a quadratic term into the established Varshni potential [7]. The introduction of an inversely quadratic term into the Varshni potential is physically motivated by the need to describe quantum systems in which short-range interactions and strong spatial confinement play a significant role [6]. The conventional Varshni potential successfully models screened interatomic and electron-ion interactions; however, it does not adequately capture singular or strongly repulsive core behaviors that arise in low-dimensional quantum systems and nanoscale structures [10]. The additional inverse-quadratic contribution introduces a centrifugal-like interaction that effectively accounts for strong localization effects near the origin, which are commonly encountered in semiconductor quantum dots, quantum rings, and impurity-bound states [6].

The objective of this to determine the eigenvalues and corresponding wave functions of the three-dimensional Schrödinger equation using the inversely quadratic Varshni potential. In this paper, Section 2 derives the approximate solution of the Schrödinger equation for the Inversely Quadratic Varshni potential, yielding analytical expressions for the energy eigenvalues and the corresponding wave functions for the quantum numbers n and l. Section 3 is devoted to a discussion of the results, and Section 4 summarizes the main conclusions. The Inversely Quadratic Varshni potentials (IQVP) is express as

$$V(r) = \left(A - \frac{ABe^{-\alpha r}}{r^2} \right) \tag{1}$$

where A and B denote the strong points of the Varshni potential, α represents the adjustable screening parameter, and r being the inter particle distance. In Figure 1(a, b), we present the behavior of the Varshni potential and the Inversely Quadratic Varshni potential as a function of different parameter values.

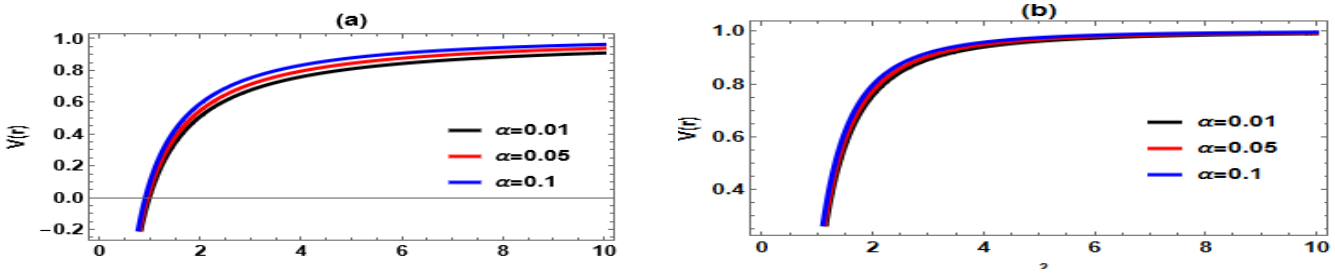

Figure 1 Variation of the Varshini potential and inversely quadratic Varshini potential with internuclear distance

Nikiforov-Uvarov-Functional Analysis (NUFA) method

The method, recently developed by Ikot *et al.* [12], has demonstrated strong effectiveness in solving wave equations involving exponential-type potentials for both relativistic and nonrelativistic systems. Its application to the Schrödinger or Klein-Gordon equation yields the energy eigenvalue equation in a compact, closed, and factorized form, offering a clear improvement over conventional analytical methods.

The methodological framework is based on solving second-order Schrödinger-like differential equations by analytically combining the Nikiforov-Uvarov (NU) method with the functional analysis approach [13, 14]. Within this scheme, the NU method is utilized to handle second-order differential equations of the form:

$$\psi''(x)+\tilde{\tau}(x)(\sigma(x))^{-1}\psi'(x)+\tilde{\sigma}(x)\left(\sigma^2(x)\right)^{-1}\psi(x)=0 \tag{2}$$

where $\sigma(x)$ and $\tilde{\sigma}(x)$ are polynomials of at most second degree, while $\tilde{\tau}(x)$ is a first-degree polynomial. Tezcan and Sever [15] later reformulated the NU method into a parametric representation given below:

$$\psi''(x)+\frac{(h_1-h_2)x}{x(1-h_3x)}\psi'(x)+\frac{1}{x^2(1-h_3x)^2}\left[-\zeta_1x^2+\zeta_2x-\zeta_3\right]\psi(x)=0 \tag{3}$$

where h_k and ζ_k are all parameters for $k=1,2,3,....$. Equation (3) possesses two singularities located at $x\to 0$ and $x\to h_3^{-1}$ consequently, the wave function can be written as.

$$\psi_n(x)=x^{\lambda}(1-h_3x)^{J}\Phi(x) \tag{4}$$

Equation (4) is substituted into Eq. (3), and after simplification, the resulting equation is given by:

$$\begin{aligned}
&x(1-h_3x)\Phi''(x)+\left[h_1+2\lambda-(2\lambda h_3+2Jh_3+h_2)x\right]\Phi'(x)\\
&-h_3\left(\lambda+J+\frac{h_2h_3^{-1}-1}{2}+\sqrt{\frac{\left(h_2h_3^{-1}-1\right)^2}{4}+\zeta_1h_3^{-2}}\right)\\
&\times\left(\lambda+J+\frac{h_2h_3^{-1}-1}{2}-\sqrt{\frac{\left(h_2h_3^{-1}-1\right)^2}{4}+\zeta_1h_3^{-2}}\right)\Phi(x)\\
&+\left[\frac{\lambda(\lambda-1)+h_1\lambda-\zeta_3}{x}+\frac{J(J-1)h_3+h_2J-h_1h_3J-\zeta_1h_3^{-1}+\zeta_2+\zeta_3h_3}{(1-h_3x)}\right]=0
\end{aligned} \tag{5}$$

Equation (5) reduces to a Gaussian hypergeometric equation provided that the functions listed below vanish:

$$\lambda(\lambda-1)+h_1\lambda-\zeta_3=0 \tag{6}$$

$$J(J-1)h_3+h_2J-h_1h_3J-\zeta_1h_3^{-1}+\zeta_2+\zeta_3h_3=0 \tag{7}$$

The solutions of Eqs. (6) and (7) are given as

$$\lambda=\frac{(1-h_1)\pm\sqrt{(1-h_1)^2+4\zeta_3}}{2} \tag{8}$$

$$J=\frac{\left(h_3+h_1h_3-h_2\right)\pm\sqrt{\left(h_3+h_1h_3-h_2\right)^2+4\left(\zeta_1h_3^{-1}+\zeta_3h_3-\zeta_2\right)}}{2h_3} \tag{9}$$

Substituting the conditions of Eqs. (6) and (7) into Eq. (5) yields Eq. (10)

$$\begin{aligned}&x\left(1-h_3x\right)\Phi''(x)+\left[h_1+2\lambda-\left(2\lambda h_3+2Jh_3+h_2\right)x\right]\Phi'(x)\\&-h_3\left(\lambda+J+\frac{h_2h_3^{-1}-1}{2}+\sqrt{\frac{\left(h_2h_3^{-1}-1\right)^2}{4}+\zeta_1h_3^{-2}}\right)\\&\times\left(\lambda+J+\frac{h_2h_3^{-1}-1}{2}-\sqrt{\frac{\left(h_2h_3^{-1}-1\right)^2}{4}+\zeta_1h_3^{-2}}\right)\Phi(x)=0\end{aligned} \tag{10}$$

Equation (10) takes the form of a hypergeometric-type equation given by

$$s\left(1-s\right)f''(s)+\left[b-\left(a_0+a_1+1\right)s\right]f'(s)-\left[a_0a_1\right]f(s)=0 \tag{11}$$

where a_0, a_1 and b are given as follows:

$$a_0=\sqrt{h_3}\left(\lambda+J+\frac{h_2h_3^{-1}-1}{2}+\sqrt{\frac{\left(h_2h_3^{-1}-1\right)^2}{4}+\zeta_1h_3^{-2}}\right) \tag{12}$$

$$a_1=\sqrt{h_3}\left(\lambda+J+\frac{h_2h_3^{-1}-1}{2}-\sqrt{\frac{\left(h_2h_3^{-1}-1\right)^2}{4}+\zeta_1h_3^{-2}}\right) \tag{13}$$

$$b=h_1+2\lambda \tag{14}$$

When either a_0 or a_1 is set to a negative integer, $\left(-n\right)$, the hypergeometric function terminates and becomes a polynomial of degree n. Consequently, the hypergeometric function remains finite under the quantum condition, i.e., $a_0=-n$ where $n=0,1,2,3,....n_{\max}$ or $a_1=-n$. Applying this condition, Eq. (12) simplifies to

$$\lambda+J+\frac{h_2h_3^{-1}-1}{2}+\frac{n}{\sqrt{h_3}}=-\sqrt{\frac{\left(h_2h_3^{-1}-1\right)^2}{4}+\zeta_1h_3^{-2}} \tag{15}$$

Equation (15) is simplified to yield the energy eigenvalue equation using the NUFA method, given by

$$\lambda^2+2\lambda\left(J+\frac{h_2h_3^{-1}-1}{2}+\frac{n}{\sqrt{h_3}}\right)+\left(J+\frac{h_2h_3^{-1}-1}{2}+\frac{n}{\sqrt{h_3}}\right)^2-\frac{\left(h_2h_3^{-1}-1\right)^2}{4}-\zeta_1h_3^{-2}=0 \tag{16}$$

Equations (8) and (9) are substituted into Eq. (4), resulting in the associated wave equation

$$\psi_n(x)=x^{\frac{(1-h_1)\pm\sqrt{(1-h_1)^2+4\zeta_3}}{2}}\left(1-h_3x\right)^{\frac{\left(h_3+h_1h_3-h_2\right)\pm\sqrt{\left(h_3+h_1h_3-h_2\right)^2+4\left(\zeta_1h_3^{-1}+\zeta_3h_3-\zeta_2\right)}}{2h_3}}{}_2F_1\left(a_0,a_1,b;x\right) \tag{17}$$

Nonrelativistic Eigen solution of Schrodinger equation with IQVP

Considering the radial Schrödinger equation for a three-dimensional system [16-18];

$$R''_{nl}(r)+\frac{2\mu}{\hbar^2}\left[E_{nl}-V(r)-\frac{\hbar^2}{2\mu}\frac{l(l+1)}{r^2}\right]R_{nl}(r)=0 \tag{18}$$

where E_{nl} denotes the approximate bound-state energy eigenvalues,, $R_{nl}(r)$ s the wave function, and μ represent the reduced mass. The quantities n and l correspond to the principal quantum number and the rotational (angular momentum) quantum number, respectively. Substituting Eq. (1) into Eq. (18) yields

$$R''_{nl}(r)+\frac{2\mu}{\hbar^2}\left[E_{nl}-\left(A-\frac{ABe^{-\alpha r}}{r^2}\right)-\frac{\hbar^2}{2\mu}\frac{l(l+1)}{r^2}\right]R_{nl}(r)=0 \tag{19}$$

The presence of the centrifugal term $\frac{1}{r^2}$ in the effective potential hinders an exact solution of Eq. (19). Therefore, the Greene–Aldrich approximation scheme [19–21] is employed, which is applicable only for small values of the screening parameter:

$$\frac{1}{r^2}\approx\frac{\alpha^2}{(1-e^{-\alpha r})^2} \tag{20}$$

By inserting Eq. (20) into Eq. (19) and applying the transformation, $z=e^{-\alpha r}$, Eq. (19) reduce to:

$$R''_{nl}(z)+\frac{(1-z)}{z(1-z)}R'_{nl}(z)+\frac{1}{z^2(1-z)^2}\begin{bmatrix}-(\varepsilon_{nl}-\delta_0)z^2+(2\varepsilon_{nl}+2\delta_0+\delta_1)z\\-(\varepsilon_{nl}+\delta_0+\eta)\end{bmatrix}R_{nl}(z)=0 \tag{21}$$

where

$$\varepsilon_{nl}=-\frac{2\mu E_{nl}}{\hbar^2\alpha^2},\ \delta_0=\frac{2\mu A}{\hbar^2\alpha^2},\ \delta_1=\frac{2\mu AB}{\hbar^2},\eta=l(l+1) \tag{22}$$

Upon comparison of Eq. (21) with the NUFA differential equation presented in Eq. (3), the resulting polynomial equations are derived:

$$\begin{aligned}&h_1=h_2=h_3=1\\&\zeta_1=(\varepsilon_{nl}-\delta_0)\\&\zeta_2=(2\varepsilon_{nl}+2\delta_0+\delta_1)\\&\zeta_3=(\varepsilon_{nl}+\delta_0+\eta)\end{aligned} \tag{23}$$

Using Eqs. (8), (9), (12), (13), and (14), the following polynomial equations can be derived:

$$\lambda=\sqrt{\varepsilon_{nl}+\delta_0+\eta} \tag{24}$$

$$J=\frac{1}{2}\pm\sqrt{\frac{1}{4}-\delta_1+\eta} \tag{25}$$

$$a_0=\left(\sqrt{\varepsilon_{nl}+\delta_0+\eta}+\frac{1}{2}\pm\sqrt{\frac{1}{4}-\delta_1+\eta}+\sqrt{\varepsilon_{nl}-\delta_0}\right) \tag{26}$$

$$a_1 = \left(\sqrt{\varepsilon_{nl} + \delta_0 + \eta} + \frac{1}{2} \pm \sqrt{\frac{1}{4} - \delta_1 + \eta} - \sqrt{\varepsilon_{nl} - \delta_0} \right) \tag{27}$$

$$b = 1 + 2\sqrt{\varepsilon_{nl} + \delta_0 + \eta} \tag{28}$$

Using Eq. (16), the energy eigen equation is obtained

$$\varepsilon_{nl} = \delta_0 - \eta + \frac{1}{4}\left[\frac{-2\delta_0 - \eta - (n+J)^2}{(n+J)} \right]^2 \tag{29}$$

By inserting the parameters of Eq. (22) into Eq. (29), the energy equation takes the form

$$E_{nl} = \frac{\hbar^2\alpha^2}{2\mu} l(l+1) - A - \frac{\hbar^2\alpha^2}{8\mu}\left[\frac{\left(n + \frac{1}{2} + \sqrt{\frac{1}{4} - \frac{2\mu AB}{\hbar^2} + l(l+1)} \right)^2 + \frac{4\mu A}{\hbar^2\alpha^2} + l(l+1)}{\left(n + \frac{1}{2} + \sqrt{\frac{1}{4} - \frac{2\mu AB}{\hbar^2} + l(l+1)} \right)} \right]^2 \tag{30}$$

The corresponding un-normalized wave function is obtained using Eq. (17)

$$R_{nl}(z) = N_{nl} z^{\lambda} (1-z)^{J} \, {}_2F_1(a_0, a_1, b; z) \tag{31}$$

where N_{nl} is the normalization constant and ${}_2F_1(a_0, a_1, b; z)$ is the hypergeometric function.
To determine the normalization constant N_{nl}, we apply the wave function's normalization condition as follows:

$$\int_{-\infty}^{\infty} |\psi_{nl}(z)|^2 dz = 1 \tag{32}$$

Put eq. (31) into (32) we obtain

$$|N_{nl}|^2 \int_0^1 I_{nl} dz = 2\alpha \tag{33}$$

where

$$I_{nl} = z^{2\lambda-1}(1-z)^{2J}\left[{}_2F_1(a_0, a_1, b; z) \right] \tag{34}$$

We evaluate the integral in eq. (34), using the Mathematica software program. Therefore,

$$N_{nl} = \sqrt{\left(\frac{2\alpha(n+\lambda+J)\Gamma(1+n+2\lambda)\Gamma(n+2\lambda+2J)}{n!(n+J)\Gamma(2\lambda)\Gamma(1+2\lambda)\Gamma(n+2J)} \right)} \tag{35}$$

Thus, the normalized wave function for the IQVP is derived as follows:

$$R_{nl}(z) = \sqrt{\left(\frac{2\alpha(n+\lambda+J)\Gamma(1+n+2\lambda)\Gamma(n+2\lambda+2J)}{n!(n+J)\Gamma(2\lambda)\Gamma(1+2\lambda)\Gamma(n+2J)} \right)} \times z^{\lambda}(1-z)^{J} \, {}_2F_1(a_0, a_1, b; z) \tag{36}$$

Thermodynamic Properties of IQVP

The thermal properties of the IQVP model are studied through the evaluation of its partition function. In a framework of canonical ensemble, the partition function is obtained by summing over the bound-state energy contributions of any system at a given temperature T [22-25];

$$Z(\beta)=\sum_{n=0}^{\varpi} e^{-\beta E_{nl}}, \quad \beta=\frac{1}{k_B T} \tag{37}$$

where n is the vibrational quantum number, $n=0,1,2,3.....\varpi$ and ϖ denotes the upper bound of the vibrational quantum number, k_B and T are Boltzmann constant and the absolute temperature, respectively. Within the classical approximation, the summation in Eq. (37) may be replaced by an integral:

$$Z(\beta)=\int_0^{\varpi} e^{-\beta E_{nl}}\, dn \tag{38}$$

Equation (30) can be rewritten in a more simplified form as

$$E_{nl}=\phi_0-\phi_1\left[\frac{\phi_3+(n+J)^2}{(n+J)}\right]^2 \tag{39}$$

where

$$\phi_0=\frac{\hbar^2\alpha^2}{2\mu}l(l+1)-A,\ \phi_1=\frac{\hbar^2\alpha^2}{8\mu},\phi_3=\frac{4\mu A}{\hbar^2\alpha^2}+l(l+1) \tag{40}$$

The maximum value of the vibrational quantum number is determined by setting the derivative of $\frac{dE_{nl}}{dn}=0$,

$$n_{\max}=-J\pm\sqrt{\phi_1} \tag{41}$$

Substitute Eq. (39) into (38), the partition function takes the form

$$Z(\beta)=\int_0^{n_{\max}} e^{-\beta\left(\phi_0-\phi_1\left[\frac{(n+J)^2+\phi_3}{(n+J)}\right]^2\right)}dn \tag{41}$$

If we set $\rho=n+J$, $\upsilon_0=J$, $\upsilon_1=\varpi+J$ and $\phi_2=\phi_0+2\phi_1\phi_3$, The integral in Eq. (41) can be rewritten as;

$$Z(\beta)=\int_{\upsilon_0}^{\upsilon_1} e^{\beta\left(\phi_2+\phi_1\rho^2+\frac{\phi_1\phi_3^2}{\rho^2}\right)}d\rho \tag{42}$$

We utilized Mathematica software to compute the integral in Eq. (42) is evaluated to obtain the partition function for the IQVP.

$$Z(\beta) = -\frac{e^{-2\sqrt{-\beta\phi}\sqrt{-\beta\phi_0\phi_3^2}-\beta\phi_2}\sqrt{\pi}\left[\hat{\Delta}_1 - \hat{\Delta}_2\right]}{4\sqrt{-\beta\phi}} \tag{43}$$

where

$$\begin{aligned}
\hat{\Delta}_1 &= Erf\left[\upsilon_0\sqrt{-\beta\phi} - \frac{\sqrt{-\beta\phi_0\phi_3^2}}{\upsilon_0}\right] + e^{4\sqrt{-\beta\phi}\sqrt{-\beta\phi_0\phi_3^2}}\, Erf\left[\upsilon_0\sqrt{-\beta\phi} + \frac{\sqrt{-\beta\phi_0\phi_3^2}}{\upsilon_0}\right] \\
\hat{\Delta}_2 &= Erf\left[\upsilon_1\sqrt{-\beta\phi} - \frac{\sqrt{-\beta\phi_0\phi_3^2}}{\upsilon_1}\right] - e^{4\sqrt{-\beta\phi}\sqrt{-\beta\phi_0\phi_3^2}}\, Erf\left[\upsilon_1\sqrt{-\beta\phi} + \frac{\sqrt{-\beta\phi_0\phi_3^2}}{\upsilon_1}\right]
\end{aligned} \tag{44}$$

Equation (43) serves as the fundamental distribution function from which various thermodynamic properties of the IQVP system are derived. These include the free energy of the system $\mathrm{F}(\beta) = -\frac{1}{\beta}\ln \mathrm{Z}(\beta)$, entropy of the system $\mathrm{S}(\beta) = -k_B\frac{\partial \mathrm{F}(\beta)}{\partial\beta}$, internal energy of the system $\mathrm{U}(\beta) = \frac{\partial \ln \mathrm{Z}(\beta)}{\partial\beta}$ and specific heat capacity of the system $\mathrm{C_V}(\beta) = k_B\frac{\partial \mathrm{U}(\beta)}{\partial\beta}$, [26, 27];

RESULT AND DISCUSSION

We employ the Nikiforov–Uvarov Functional Analysis (NUFA) method to obtain solutions of the radial Schrödinger equation in three dimensions for the Inversely Quadratic Varshni potential. The closed-form expression for the energy eigenvalues is obtained in Eq. (30), and the corresponding normalized wave function is provided in Eq. (36). The energy eigenvalues of the system are computed using the chosen arbitrary parameters $\hbar = \mu = A = B = 1$ as summarized in Tables 1 and 2. Table 1 shows the calculated bound-state energies of the Inversely Quadratic Varshni potential (IQVP) corresponding to different values of the screening parameter α. For all considered cases, the energy eigenvalues are observed to rise with increasing quantum numbers n and l. Table 2 shows the energy eigenvalues of the Varshni potential (VP). The results indicate that the energy rises with increasing quantum numbers and remains higher for all considered parameter values of α.

Table 1 ***Energy eigenvalues of Inversely Quadratic Varshni (IQV) potentials***

n	l	$\alpha = 0.01$	$\alpha = 0.05$	$\alpha = 0.1$
0	0	1.00002	1.00047	1.00188
1	0	0.999994	0.999844	0.999375
2	0	0.999944	0.998594	0.994375
	1	0.999988	0.999688	0.99875
	0	0.999869	0.996719	0.986875
3	1	0.999847	0.996172	0.984688
	2	0.999749	0.99372	0.974882
	0	0.999769	0.994219	0.976875
4	1	0.999736	0.993388	0.97355
	2	0.999601	0.990034	0.960137
	3	0.999528	0.988206	0.952823
	0	0.999644	0.991094	0.964375
5	1	0.999599	0.989965	0.959861

2	0.999427	0.985685	0.942742
3	0.99933	0.983244	0.932976
4	0.999254	0.98135	0.925399

Table 2 ***Energy eigenvalues of Inversely Quadratic Varshni potentials***

n	l	$\alpha = 0.01$	$\alpha = 0.05$	$\alpha = 0.1$
0	0	0.504987	0.524688	0.54875
1	0	0.87995	0.89875	0.92
2	0	0.949332	0.966632	0.983194
	1	0.882488	0.912187	0.94875
	0	0.97355	0.98875	0.99875
3	1	0.985135	1.00039	1.00755
	2	0.991632	1.00747	1.01319
	0	0.984688	0.997188	0.99875
	1	0.990988	1.00247	0.99875
4	2	0.994936	1.00607	0.99875
	3	0.997597	1.00867	0.99875
	0	0.990661	0.999861	0.991111
	1	0.994436	1.00173	0.985485
5	2	0.996999	1.00311	0.981172
	3	0.998833	1.00416	0.977762
	4	1.0002	1.005	0.975

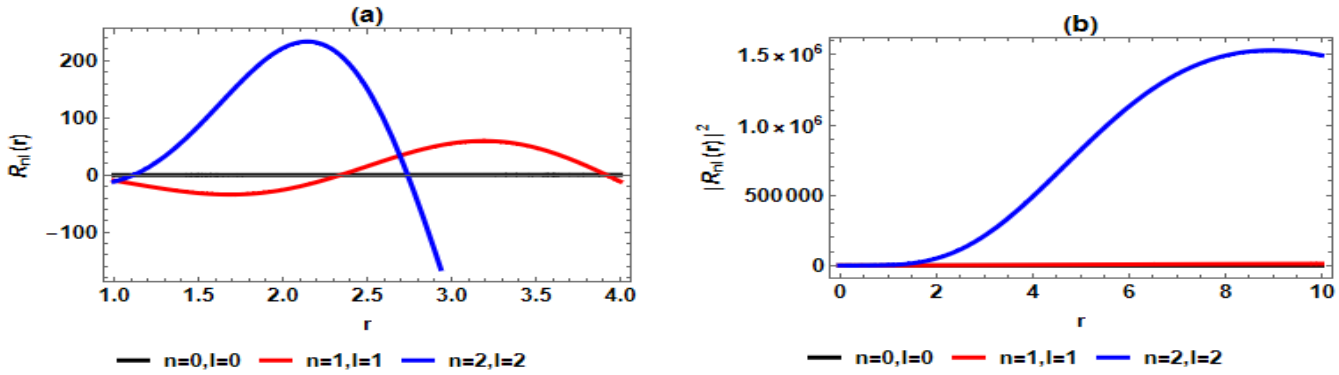

Fig. 2 Variation of the radial wave function and the corresponding probability density with radial distance

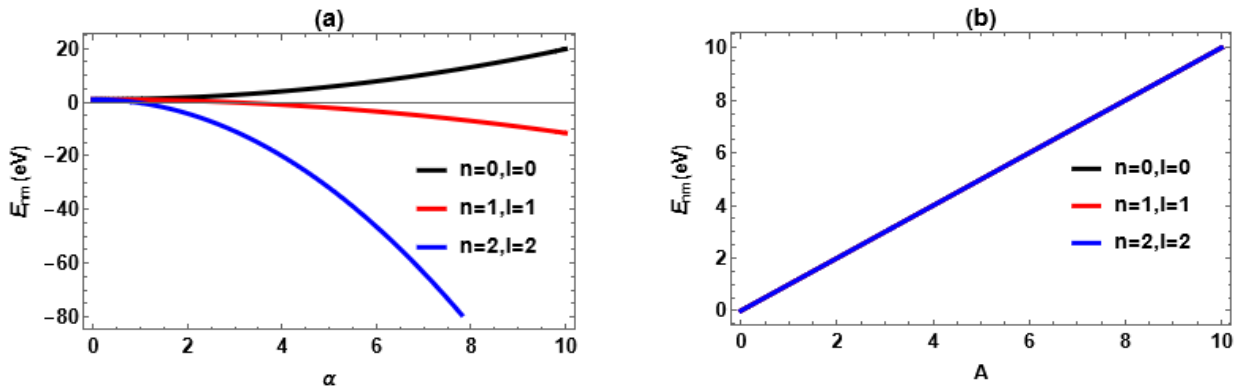

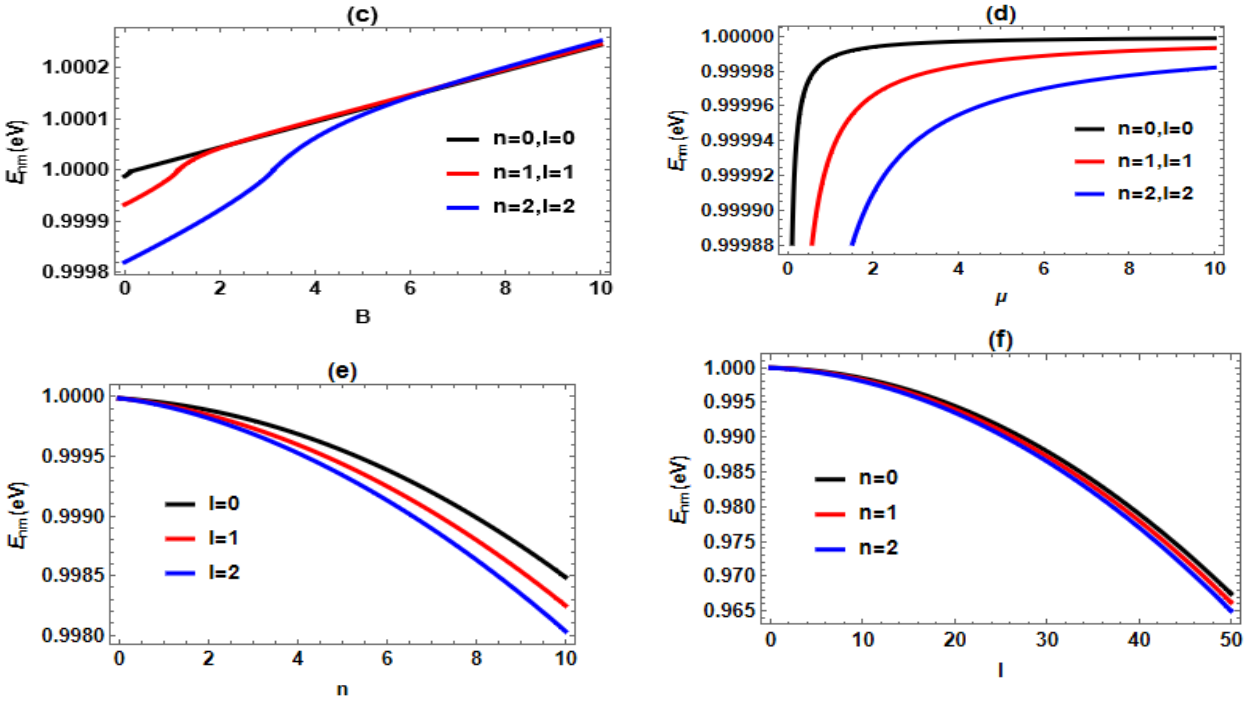

Fig. 3 Energy variation of the IQV potential as a function of (a) the screening parameter, α (b, c) the potential strength parameter, A and B (d) the reduced mass (e, f) quantum numbers, n and l

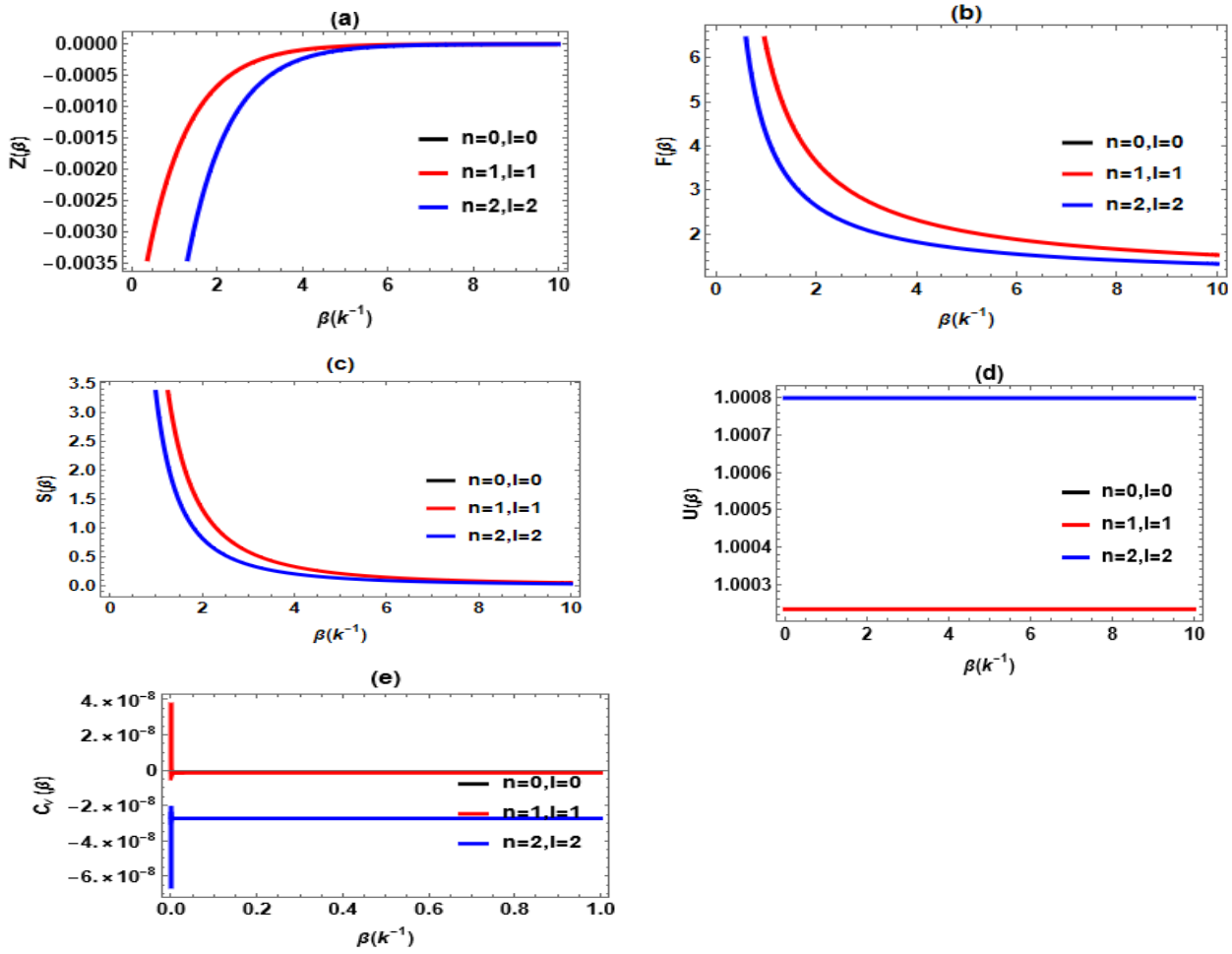

Fig. 4 Thermodynamic properties of the IQV potential as a function of inverse temperature

Figure 1(a) presents the Varshni potential as a function of the internuclear distance, r, whereas Fig. 1(b) displays the inversely quadratic Varshni potentials. The IQVP shows a behavior closely matching that of the Varshni potential. Accordingly, a particle confined in the IQVP is subject to the effects of the Varshni potential to a greater extent. In Fig. 2(a, b), the radial wave function and corresponding probability density for the low- and high-lying states are plotted against the radial distance, r, with the quantum numbers n and l varying accordingly. Notably, the high-lying states are more concentrated and show increased localization relative to the low-lying states. The peaks of the radial wave function and probability density in both cases are observed to decrease with increasing radial distance, r. Moreover, for both cases, the radial wave function and probability density display a sinusoidal behavior as r increases, while the probability density tends toward zero. In Fig. 3(a), the energy of the IQVP is plotted against the adjustable screening parameter, α, for several values of the quantum numbers n and l. For higher quantum numbers n and l the energy decreases as α increase while at lower quantum numbers n and l it remains unchanged. In Fig. 3(b), the energy exhibits to increase linearly with the potential parameter A. A similar trend is seen in Fig. 3(c), where the energy rises with the parameter B. In Fig. 3(d), the energy is seen to increase monotonically with the reduced mass μ. In Figs. 3(e) and 3(f), the energy decreases linearly with increasing principal and orbital quantum numbers, n and l, respectively.

In Fig. 4(a), the vibrational partition function, $Z(\beta)$ is illustrated with respect to temperature $\beta(k^{-1})$, or selected quantum numbers n and l. For all cases, the partition function increases initially and then saturates, indicating that the likelihood of the system occupying a particular microstate grows at first and becomes constant as $\beta(k^{-1})$, increases. This behavior is consistent with classical thermodynamics, as an increase in temperature raises the energy of the system and, consequently, the number of accessible microstates. In Fig. 4(b), the free energy, $F(\beta)$, exhibits an inverse relationship with temperature $\beta(k^{-1})$, as free energy $F(\beta)$ decreases monotonically with increasing $\beta(k^{-1})$. In Fig. 4(c), the vibrational entropy $S(\beta)$, exhibits a trend similar to that observed for the free energy in Fig. 4(b). In Fig. 4(d), the internal energy $U(\beta)$ remains nearly constant as the temperature $\beta(k^{-1})$ increases. A similar behavior is observed for the vibrational specific heat $C_v(\beta)$ of the system in the same Fig. 4(e). This is governed by the interplay between thermal excitation and the modified energy spectrum generated by the combined screening and inverse-square confinement features of the IQVP.

CONCLUSION

In this study, the Schrödinger equation for the Inversely Quadratic Varshni Potential (IQVP) is solved using the NUFA method. The solutions obtained are further utilized to analyze the thermodynamic properties of the system, and the resulting numerical data are presented. The observed trends in the thermodynamic plots agree well with prior studies [26, 32], thereby confirming the reliability of the analytical results obtained here. From these findings, it is concluded that the IQVP provides a realistic and flexible potential model with potential applications across atomic, molecular, and nuclear physics.

ACKNOWLEDGMENTS

The authors wish to express their sincere gratitude to the National Mathematical Centre, Abuja, for their support.

DISCLOSURE STATEMENT

The author(s) report no potential conflicts of interest.

REFERENCES

[1] Ukewuihe, U. M., Onyenegecha, C. P., Udensi, S. C., Nwokocha, C. O., Okereke, C. J., Njoku, I. J., & Iloanya, A. C. (2021). Approximate solutions of Schrodinger equation in D-Dimensions with the modified Mobius square plus Hulthen potential. *Mathematics & Computational Science*, 2 (2), 1-15. https:// doi. org/ 10.30511/mcs.2021.527027.1020

[2] Ahmadov, A. L., Aslanova, S. M., Orujova, M. Sh., Badalov, S.V., & Dong, S. H. (2019). Approximate bound state solutions of the Klein Gordon equation with the linear combination of Hulthén and Yukawa potentials.*Physics Letter A,* 383(24), 3010 3017.

[3] Hassanabadi, A., Ikot, A. N., Onyenegecha, C. P., & Zarrinkamar, S. (2017). Approximate bound and scattering solutions of Dirac equation for the modified deformed Hylleraas potential with a Yukawa-type tensor interaction. *Indian Journal of Physics,* 91(9), 1103-1113.

[4] Oyewumi, C. P., & Oluwadare, O. J. (2016). The scattering phase shifts of the Hulthén-type potential plus Yukawa potential. *The European Physical Journal Plus*, 131(9), 1-10.

[5] Taskin, F., & Kocak, G. (2010). Approximate solutions of Schrödinger equation for Eckart potential with centrifugal term. *Chinese Physics B*, 19 (9), 090314.

[6] Imrana, M. H., Yabagi, J. A., Teru, P. B., Ngari, A. Z., Adamu, Y., Ubaidullah, A., & Gene, S. (2025). Energy spectrum and partition function of the Varshni-Hellmann potential in the presence of magnetic and AB flux fields. *Indian Journal of Physics*. https://doi.org/10.1007/s12648-025-03842-3

[7] Tazimi, N., & Sadeghi Alavijeh, P. (2021). Investigation of baryons in the hypercentral quark model, *Advances in High Energy Physics*. Article ID 7713697, 11.

[8] William, E. S., Inyang, E. P., & Thompson, E. A. (2020). Arbitrary l solutions of the Schrödinger equation interacting with Hulthén-Hellmann potential model, *Revista Mexicana de Física*. 66,730–741.

[9] Hellmann, H. (1935). A new approximation method in the problem of many electrons, *Journal of Chemical Physics*. 3(1), 61–61.

[10] Edet, C. O., Okorie, U. S., Ngiangia, A. T., & Ikot, A. N. (2020) . Bound state solutions of the Schrodinger equation for the modified Kratzer potential plus screened Coulomb potential, *Indian Journal of Physics*. 94 (4), 425–433.

[11] Oluwadare, O. J., & Oyewumi, K. J. (2017). The semi-relativistic scattering states of the two-body spinless Salpeter equation with the Varshni potential model, *The European Physical Journal Plus*. 132 (6), 277.

[12] Ikot, A. N., Okorie, U. S., Amadi, P. O., Edet, C. O., Rampho, G. J., & Sever, R. (2021). The Nikiforov-Uvarov-Functional analysis (NUFA) method: A new Approach for soling exponential type potentials. *Few-Body System,* 62, 9. https://doi.org/10.1007/s00601-021-01593-5

[13] Ikot, A. N., Awoga, O.A., & Antia, A. D. (2013). Bound state solutions of d-dimensional Schrodinger equation with Eckart potential plus modified deformed Hylleraas potential. , *Chinese Physics B,* 22, 020304.

[14] Falaye, B. J., Ikhdair, S. M., & Hamzavi, M. (2015). Formula method for bound state problems. *Few-Body System,* 56, 63.

[15] Tezcan, C., & Sever, R. (2009). A general approach for the exact solution of the Schrodinger equation, *International Journal of Theoretical Physics*. 48, 337.

[16] Mathe, L., Onyenegecha, C. P., Farcas, A. A., Pioras- Timbolmas, L. M., Solaimani, M., & Hassanabadi, H. (2021). Linear and nonlinear optical properties in spherical quantum dots: Inversely quadratic Hellmann potential. *Physics Letter A*, 397 127262.

[17] Onyenegecha, C. P., Ukewuihe, U. M., Opara, A. I., Agbakwuru, C. B., Okereke, C. J., Ugochukwu, N. R., Okolie, S. A., & Njoku, I. J. (2020). Approximate solutions of Schrodinger equation for the Hua plus modified Eckart potential with the Centrifugal, *The European Physical Journal Plus*. 135(7), 1-10.

[18] Ikot, A. N., Rampho, G. J., Amadi, P. O., Sithole, M. J., Okorie, U. S., & Lekala, M. I. (2020). Shannon entropy and Fisher information theoretic measures for Mobius square potential. *The European Physical Journal Plus,* 135(6), 1-13.

[19] Greene, R. L., & Aldrich, C. (1976). Variational wave functions for a screened Coulomb potential. *Physics Reviews A*. 14(6), 2363.

[20] Imrana, M. H., Ngari, A. Z., Teru, P. B., Gyobe, A. M., Ndom, N. B., Yabagi, J. A., & Ndanusa, B. (2025). Thermo-Magnetic properties of Two-Dimensional Non-Relativistic Schrödinger Equation for the Attractive Radial Potential under External Magnetic and Aharonov-Bohm Flux Fields. *Nigerian Journal of Theoretical & Environmental Physics*, 3(4), 45-60. https://doi.org/10.62292/njtep.v3i4.2025.102

[21] Ikot, A. N., Zarrinkamar, S., Ibanga, E. J., Maghsoodi, E., & Hassanabadi, H. (2014). Pseudospin symmetry of the Dirac equation for a Möbius square plus Mie type potential with a Coulomb-like tensor interaction via SUSYQM. *Chinese Physics C*, 38(1), 013101.

[22] Omugbe, E., Osafile, O. E., Okon, I. B., & Onyeaju, M. C. (2020). Energy Spectrum and the properties of the Schiöberg potential using the WKB approximation approach. *Molecular Physics*, 119, e1818860. https:// doi. org/ 10. 1080/ 00268 976. 2020. 18188 60

[23] Okon, I. B., Onate, C. A., Horchani, R., Popoola, O. O., Omugbe, E., William, E. S., Okorie, U. S., Inyang, E. P., Isonguyo, C. N., Udoh, M. E., Antia, A. D., Chen, W. L., Eyube, E. S., Araujo, J. P., & Ikot, A. N. (2023). Thermomagnetic properties and its effects on Fisher entropy with Schioberg plus Manning-Rosen potential (SPMRP) using Nikiforov-Uvarov functional analysis (NUFA) and supersymmetric quantum mechanics (SUSYQM) methods. *Scientific Report*, 13, 8193. https://doi.org/10.1038/s41598-023-34521-0

[24] Yazarloo, B. H., & Mehraban, H. (2017). Relativistic bound and scattering amplitude of spinless particles in modified Schioberg Plus Manning-Rosen potentials. *Communication in Theoretical Physics*, 67, 71. https:// doi. org/ 10. 1088/ 0253- 6102/ 67/1/ 71

[25] Ikot, A. N., Hassanabadi, H., Obong, H. P., Mehraban, H., & Yazarloo, B. H. (2015). Approximate arbitrary κ-state solutions of Dirac equa tion with Schiöberg and Manning-Rosen potentials within the coulomb-like Yukawa-like and generalized tensor interactions. *Physics Particle & Nuclear Letter*, 12, 498–515. https:// doi.org/ 10. 1134/ S1547 47711 50401 59

[26] Wang, P. Q., Liu, J. Y., Zhang, L. H., Cao, S. Y., & Jia, C. S. (2012). Improved expressions for the Schiöberg potential energy models for diatomic molecules. *Journal of Molecular Spectroscopy*, 278, 23 https:// doi. org/ 10. 1016/j. jms. 2012. 07. 001

[27] Hassanabdi, A., Yazarloo, B. H., Zarrinkamar, S. S., & Rahimov, H. (2012). Spin and Pseudospin Symmetries of Dirac Equation and the Yukawa Potential as the Tensor Interaction. *Communication in Theoretical Physics,* 58(6), 807.

[28] Ikot, A. N., Awoga, O. A., Hassanabadi, H., & Maghsoodi, E. (2014). Analytical approximation solution of Schrodinger equation in D-Dimensions with Quadratic exponential type potential for arbitratry l-state, *Communication in Theoretical Physics,* 61(4), 457.

[29] Niknam, A. Rajabi, A. A., & Solaimani, M. (2016). Solutions of D-dimensional Schrodinger equation for Woods-Saxon potential with spin-orbit, coulomb and centrifugal terms through a new hybrid numerical fitting Nikiforov-Uvarov method. *Journal of Theoretical & Applied Physics*, 10(1), 53-59.

[30] Jia, C. S., Zeng, R., Peng, X. L., Zhang, L. H., & Zhao, Y. L. (2018). Entropy of gaseous phosphorus dimer. *Chemical Engineering Science*, 190, 1–4

[31] Habibinejad, M., & Ghanbari. A. (2021). Enthalpy, Gibbs free energy and specific heat in constant pressure for diatomic molecules using improved deformed exponential-type potential (IDEP). *The European Physical Journal Plus,* 136, 400

[32] Hoi, B. D., Tung, L. V., Vinh, P. T., Khoa, D. Q., & Phuong, L. T. (2021). Electric field and charged impurity doping effects on the Schottky anomaly of β 12-borophene. *Physics Chemistry*, 23, 2080–2087

[33] Edet, C. O., & Ikot, A. N. (2021). Analysis of the impact of external fields on the energy spectra and thermo-magnetic properties of N_2, I_2, CO, NO and HCl diatomic molecules. *Molecular Physics,* 119, e1957170